Journal Pre-proof

The use of UV/H_2O_2 to facilitate removal of emerging contaminants in anaerobic membrane bioreactor effluents

Nicolas Augsburger [1, 2], Noor Zaouri [1], Hong Cheng [1, 2], Pei-Ying Hong [1, 2 *]

1. Water Desalination and Reuse Center, Division of Biological and Environmental Science and Engineering, King Abdullah University of Science and Technology (KAUST), 23955-6900 Thuwal, Saudi Arabia
2. Center of Excellence for NEOM Research, King Abdullah University of Science and Technology (KAUST), 23955-6900 Thuwal, Saudi Arabia

*** Corresponding author**

Email: peiying.hong@kaust.edu.sa

Telephone: +966 12 8082218

Journal Pre-proof

Journal Pre-proof

Abstract

Effluent from anaerobic membrane bioreactor (AnMBR) contains ammonia and would require post-polishing treatment before it can be disinfected by chlorine. However, additional post-treatment steps to remove nutrients offset the energetic benefits derived from anaerobic fermentation. The use of chlorine or ozone also promotes concerns associated with disinfection byproducts. This study evaluates UV/H_2O_2 as a potential strategy suited for the removal of pharmaceutical compounds as well as antibiotic resistant bacteria (ARB) and antibiotic resistance genes (ARGs) from AnMBR effluent. Our findings indicate that 10 mg/L H_2O_2 and 61.5 mJ/cm^2 of UV fluence are able to achieve a 4-log removal of both *Escherichia coli* PI7 and *Klebsiella pneumoniae* L7. However, a higher fluence of 311 mJ/cm^2 with the same amount of H_2O_2 would be required to achieve > 90% removal of atenolol, carbamazepine and estrone. The removal of the pharmaceutical compounds was driven by the hydroxyl radicals generated from H_2O_2, while UV exposure governed the inactivation of ARB and ARGs. UV/H_2O_2 increased overall mutagenicity of the treated wastewater matrix but did not result in any changes to the natural transformation rates. Instead, UV significantly reduced natural transformation rates by means of DNA damage. Overall, UV/H_2O_2 could be the ideal final disinfection strategy for AnMBR effluent without requiring additional post-treatment prior disinfection.

Keywords: Advanced oxidation processes, anaerobic membrane bioreactor, tertiary wastewater treatment, contaminants of emerging concern, pharmaceutical compound degradation

Journal Pre-proof

1. Introduction

Agriculture irrigation currently accounts for approximately 70% of global freshwater withdrawals (WWAP, 2015; 2019). A continuing trend in such unsustainable use of freshwater will exacerbate water scarcity in arid regions like the Middle East and Africa. Reusing treated wastewater for agricultural irrigation is a potential solution to alleviate the demand on freshwater supplies. Regulatory agencies in Middle East and Africa recommend guidelines devised from World Health Organization or International Organization for Standardization by listing permissible limits of fecal coliforms, biochemical oxygen demand, total suspended solids and turbidity in treated wastewater to be used for irrigation (Al-Jasser, 2011). However, emerging contaminants such as the presence of residual antibiotic-resistant bacteria (ARB), antibiotic resistance genes (ARG) and pharmaceuticals in treated wastewater effluent are not addressed in the current guidelines. An increase in wastewater reuse could aid in the dissemination of antibiotic resistance, while many chemicals of emerging concern have been shown to accumulate in a variety of crops irrigated with treated wastewater (Goldstein et al., 2014; Malchi et al., 2014; Wu et al., 2014). These observations arise due to an inconsistent removal of contaminants by conventional wastewater treatment plants (WWTP) that rely on secondary treatment processes (Verlicchi et al., 2012). There is therefore a need to enhance the removal of the aforementioned contaminants through tertiary treatment, particularly by means of membrane filtration (Kim et al., 2014) and chemical oxidation of wastewater (Okuda et al., 2008).

Microfiltration or ultrafiltration membrane bioreactors (MBR) are being considered as tertiary treatment technologies as the coupling of membrane to activated sludge processes act as an additional physical barrier that can improve effluent quality by removing particulates based on size exclusion or by adsorbing particulates on the membrane biofoulant layer (Cheng and

Journal Pre-proof

Hong, 2017; Kim et al., 2014). To exemplify, MBRs achieve 1-3 log higher removal of ARG compared to secondary activated sludge processes (Munir et al., 2011). The use of membrane filtration also eliminates the need for clarifiers, hence decreasing the required land footprint and facilitating installation of WWTP in a decentralized operation. Conventionally, MBR is operated in aerobic mode but this is an energy intensive process. Furthermore, aerobic MBR generates a large volume of solid wastes (i.e., sludge) concentrated with contaminants that would need to be properly disposed. In recent years, anaerobic MBR (AnMBR) has been explored as a more sustainable way to treat wastewater because of the recovery of methane as an energy source and a low sludge volume production.

Regardless of the type of membrane bioreactor, a final disinfection step can be utilized to complement the upstream treatment in inactivating bacteria and other contaminants, hence augmenting the final cumulative log removal of contaminants. Chlorine is a common disinfectant used in treated wastewaters. However, chlorination is ineffective in the removal of chemicals of emerging concerns (CECs) (Choi et al., 2006; Lei and Snyder, 2007) and in controlling antibiotic resistance (Fiorentino et al., 2015; Yuan et al., 2015). The use of chlorine also results in the formation of hazardous disinfection byproducts (DBPs) (Bond et al., 2011; Huang et al., 2016; Park et al., 2016; Yang et al., 2010) that are mutagenic and can trigger competent bacteria to gain new genetic materials via natural transformation (Mantilla-Calderon et al., 2019). Furthermore, AnMBR effluent is not suited to be disinfected directly with chlorine because AnMBR effluent is inherently ammonia-rich and likely to result in the formation of nitrogenous DBPs upon formation of chloramines (Shah and Mitch, 2012), which are highly toxic even in minute concentrations (Hrudey, 2009; Nieuwenhuijsen et al., 2000). This implies that the use of AnMBR to treat municipal wastewater for reuse would require further downstream nitrification

Journal Pre-proof

and denitrification biological systems prior to chlorine disinfection. However, the need for downstream nutrient removal treatment increases the footprint of AnMBR, in turn making AnMBR less appealing as a decentralized treatment technology. It also eliminates the possibility of using high quality treated wastewater as a potential liquid fertilizer for food production.

In contrast with chlorine, UV is able to efficiently inactivate microorganisms due to dimerization of pyrimidine bases in DNA when energy is absorbed in the UV-C range (Doetsch et al., 1995; Sinha and Häder, 2002). UV can also impede possible horizontal gene transfer via conjugation (Guo et al., 2015) and natural transformation (Augsburger et al., 2019; He et al., 2019; McKinney and Pruden, 2012; Yoon et al., 2018) without generating disinfection byproducts. However, UV alone via photolysis cannot proficiently remove CECs, hence there is a need to supplement an oxidant such as H_2O_2 which has been shown to enhance the removal of pharmaceutical compounds in combination with UV (Kim et al., 2009; Lee et al., 2016; Miklos et al., 2018). UV/H_2O_2 advanced oxidation process (AOP) is therefore proposed as a treatment option for the removal of CECs from ammonia-rich AnMBR effluent. Ammonia is ~97% transparent to the monochromatic light emitted by low-pressure UV lamps (254_{nm}) (Ling et al., 2011; 2013), and hence the UV would be transmitted through the water matrix effectively to inactivate ARG and ARB. UV can also react with H_2O_2 to generate hydroxyl radicals that degrade pharmaceutical compounds. To the best of our knowledge, UV/H_2O_2 has not been demonstrated for the treatment of AnMBR effluent.

This study therefore aims to demonstrate the efficacy of UV/H_2O_2 in removing both biological and chemical contaminants from an ammonia-rich effluent collected post-AnMBR. The AnMBR effluent was spiked with two pathogenic ARB (*Escherichia coli* PI-7 and *Klebsiella pneumoniae* L7) and their associated plasmid-borne ARGs (bla_{NDM-1} and $bla_{CTX-M-1}$) as

Journal Pre-proof

well as three pharmaceutical compounds (estrone, carbamezapine, and atenolol) commonly detected in wastewater effluent. The removal of these contaminants was monitored upon exposure to UV/H_2O_2 so as to determine the needed UV fluence and H_2O_2 concentration to achieve a 90% removal of the chemical contaminants and 4-log removal of the ARBs. Changes in mutagenicity level and natural transformation frequencies were also monitored to determine if UV/H_2O_2 would provide a safe means of disinfecting the wastewater.

2. Materials and methods

2.1 Anaerobic MBR (AnMBR) setup and parameters

The AnMBR operated in this study was of similar configuration to that operated in an earlier study (Cheng et al., 2019). Briefly, the AnMBR was filled with cylindrical ceramic packing medium of 1.5 cm diameter, with a 2 L working volume. Sludge was originally seeded with a mixture of camel manure and anaerobic sludge from a wastewater treatment plant in Riyadh, Saudi Arabia. The reactor was fed with municipal wastewater collected from KAUST wastewater treatment plant and operated at 35 °C (mesophilic conditions) and pH 7. Prior to feeding into the AnMBR, the influent stream is added with sodium acetate and starch to adjust the COD to approximately 800 mg/L. The organic loading rate (OLR) was hence maintained at approximately 0.69 g COD L^{-1} day^{-1}. External cross-flow flat sheet polyvinylidene difluoride (PVDF) microfiltration (MF) membrane (GE Osmonics, Minnetonka, MN, USA) was connected to the anaerobic fermentation tank to form AnMBR. The membranes had a nominal pore size of 0.3 μm. The flux was maintained at approximately 7 L/m^2/h (LMH) with an average hydraulic retention time (HRT) of 27.8 h. No sludge was wasted throughout the study. Biogas was used to

Journal Pre-proof

scour the membrane surface at a gas sparging rate of 300 mL/min and the total recirculation rate of AnMBR was maintained at 600 mL/min. The AnMBR has an average 96% COD removal throughout the study and produced an average 219 mL CH_4 per g COD. AnMBR effluent was collected daily and stored in sterile containers placed at 4 ^{o}C prior to use for inactivation experiments.

2.2 Effluent sample preparation

Fresh stocks of atenolol, carbamazepine, and estrone, each of 10 mg/mL, were prepared less than 7 d prior to UV/H_2O_2 experiments. Carbamazepine and atenolol were dissolved in the same vial containing methanol as solvent, while 1:1 methanol-water (v/v) was used to dissolve estrone. AnMBR effluent was further filtered through 0.45 μm filter prior to spiking in with tested contaminants. The effluent was spiked with each chemical to achieve final individual concentrations of 50 μg/L. The spiked concentrations for these chemicals are 223-, 41- and 37-fold greater than concentrations reported in wastewater influent for estrone, atenolol, and carbamazepine, respectively (Krzeminski et al., 2019; Subedi and Kannan, 2015). The chemicals were spiked at high concentrations to facilitate detection based on protocols described in section 2.4.

Effluents were also spiked with ARB and ARG. To prepare the ARB, a single colony of *E. coli* PI-7 and *K. pneumoniae* L7, isolated and characterized in earlier studies (Mantilla-Calderon et al., 2016; Toh et al., 2017), were individually inoculated into sterile 50 mL LB broth supplemented with either 10 μg mL^{-1} of meropenem (*E.coli* PI-7*)* or 8 μg mL^{-1} of ceftazidime (*K. pneumoniae* L7). These ARB were used because they are carbapenem-resistant and extended spectrum beta-lactamase-producing Enterobacteriaceae, and are listed as priority pathogens of

Journal Pre-proof

concern by World Health Organization (WHO, 2017). The culture was incubated overnight at 37 °C and 200 rpm, and subsequently centrifuged at 5000 *g* for 10 min. The pelleted cells were washed with 1X PBS, recentrifuged at 5000 *g* for 10 min, and the procedure was repeated twice. The washed cells were then concentrated and adjusted to a stock concentration of ca. 10^{10} cells/mL based on OD_{600nm} readings, and subsequently spiked into the AnMBR effluent. The final cellular concentrations were ca. 10^9 cells/mL for the disinfection assays. To prepare ARG, bla_{NDM-1} and $bla_{CTX-M-15}$ genes, responsible for meropenem and ceftazidime, respectively, were amplified from plasmids extracted from *E. coli* PI-7 and *K. pneumoniae* L7, respectively, using the primers in Table S1. After running a PCR, stock concentrations of 10^{14} copies/mL of each gene were obtained and subsequently spiked into the AnMBR effluent prior to AOP treatment for final concentrations of 10^9 copies/mL. All disinfection experiments described in section 2.3 were conducted in reactors containing the CECs, ARB, and ARG.

2.3 Disinfection experiments for AnMBR effluent

UV disinfection was performed using an 8 W monochromatic UVP lamp emitting light in the germicidal UV-C (254 nm) wavelength (Analytik Jena, Upland, CA). The samples were placed 14.5 cm from the lamp, which resulted in 0.55 mW/cm^2 of average irradiance at 254 nm, measured with an SU-100-SS UV sensor (Apogee Instruments, Santa Monica, CA). The emitted irradiance was calculated by multiplying the fluence rate by exposure time (Bolton and Linden, 2003). Microcosms used for UV-C_{254nm} experiments were placed within 250 mL glass beakers, each with a diameter and height of 6.5 and 9.2 cm, respectively. Correction factors taking sample depth and 254 nm transmittance into consideration were calculated to determine average UV intensity throughout the sample. Only irradiances corrected for water quality and sample depth are reported, with further details presented in Supporting Information Text 1. Spiked AnMBR

effluent samples were added into the reactors and mixed gently by a magnetic stir bar at 300 rpm, the temperature was maintained at 32 °C with a water bath. Before each experiment, the UV lamp was warmed up for 5 min to ensure stable UV radiation fluence. The disinfection experiments were carried out with 0, 10 mg/L, and 30 mg/L of H_2O_2, and up to 311 mJ/cm^2. Each disinfection test was done in technical duplicates and with at least three biological replicates.

2.4 Detection of chemical contaminants

Degradation of atenolol, carbamazepine, and estrone was monitored throughout the UV/H_2O_2 treatment. Prior to detection, a solid-phase extraction (SPE) was run on 200 mL samples exposed to 0, 52, 104, 207, and 311 mJ/cm^2 using an HLB Oasis column. The operating conditions for SPE are listed in Table S2. The final eluate from SPE of each sample was subsequently evaporated using the TurboVAP LV system at 65 ^oC with constant N_2 gas flow. After complete evaporation, each sample was resuspended in 500 µL of methanol, which was used for further detection and analysis with LC/MS.

The chromatographic separation of compounds in Alginate 1260 Infinity system was performed with a C18 column with 5 µm pore size (150 x 20 mm dimension) that was further fitted with guard column. A binary gradient of 0.1% ammonium hydroxide buffer, 4 mM ammonium formate in 0.1 % formic acid (mobile phase A) and 4 mM ammonium formate in methanol containing 0.1 % formic acid (mobile phase B) was used to provide the needed gradient for compounds separation (Table S3). The flow rate was set at 800 µL/min for 20 min running time. The mass spectrometer used was AB SCIEX QTRAP 5500. The analytes were detected using multiple reaction monitoring (MRM) in negative mode. Detailed information on the MRM transition for each chemical were provided in Table S4. The extraction efficiencies from the

Journal Pre-proof

Journal Pre-proof

AnMBR effluent were 92% ± 6%, 84% ±4%, and 93% ±4% for atenolol, carbamazepine and estrone, respectively. Standard curves for each CECs are shown in Figure S1.

2.5 Inactivation kinetics of ARB and ARG

Decay kinetics of the ARB were determined based on cell counts quantified over time through LB agar. Log removal values (LRV) were calculated using the formula of $\log_{10}(N/N_o)$, where N = CFU x dilution factor and N_o= initial cellular concentration. The ARGs were quantified via qPCR using specific target primers and probes, listed in Table S1. The qPCR assays were conducted with an Applied Biosystems 7900HT Fast real-time polymerase chain reaction (qPCR) System (Thermo Fisher Scientific, Carlsbad, CA). The qPCR standard curve was produced as previously described (Cheng and Hong, 2017) by diluting in series to obtain concentration ranging from 10^2 to 10^8 copies/µL. Each 20 µL reaction volume consisted of 10 µL Taqman fast master mix, 1 µL of each primer (10 µM), 0.8 µL respective probe, 1 µL of DNA template and 6.2 µL molecular grade H_2O. The thermal cycling profile was as follows: 50 °C for 2 min, 95 °C for 20 s, and 40 cycles of 95 °C for 1 s, 60 °C for 20 s. The standard curve and no-template controls (NTC) were performed in triplicate, while test amplifications were performed in duplicate. The amplification factor of the standards ranged from 1.89 to 2.04. All the *R*-squared values of trendlines were > 0.94 and all the NTCs have C_q values > 34. Inactivation was presented as LRV using the formula of $\log_{10}(N/N_o)$, where N= copies/µL obtained at that sampling point and N_o = the initial copies/µL upon spiking.

2.6 Evaluation of mutagenicity levels

A modified Ames reversion assay in the tester strain *Salmonella enterica* serovar Typhimurium was used to gauge toxicity of concentrated effluent as previously described (Maron and Ames, 1983). *Salmonella enterica* serovar Typhimurium TA100 and TA98 were used for mutagenicity

tests; this assay is considered the gold standard for assessing mutagenicity in bacterial systems caused from substitution/point (TA 100) and frameshift (TA 98) mutations. A 400X organic fraction concentrate stock of UV/H_2O_2-treated water was generated from solid phase extraction. Subsequently, 50 µL of stock was added to 950 µL of the cellular suspension for the final concentration of 20X treated water. Concentrates were generated from spiked AnMBR effluent after 52, 104, 207, and 311 mJ/cm^2. The mutagenicity protocol was carried out by using with a standardized ca. 10^9 cells mL^{-1} of the tester strain (determined based on OD_{600nm} measurements), incubated at 37°C with 20X concentrate of treated water for 1 h. Subsequently, 100 µL of the standardized cell solution of each strain was plated in Vogel-Bonner (VB) minimal medium. Both strains contain mutations preventing histidine synthesis, inhibiting growth in the minimal medium. Colonies that are able to grow in this minimal medium agar plates represent a reversion of these mutations due to exposure to a mutagen. The histidine revertant colonies were enumerated by colony forming unit counts on agar plates after 72 h of incubation at 37 °C. The results were expressed as fold changes, which was determined by normalizing the revertant counts by the negative control of 50 µL PPB for every mutagenicity assay. Each condition was tested with biological triplicates.

2.7. Evaluation of extracellular DNA integrity

To evaluate the changes in the extracellular DNA integrity after the proposed disinfection strategy, natural transformation assays were done using the reporter strain of *A. baylyi* ADP1 (BD413) along with its extracellular donor DNA (Rizzi et al., 2008). Briefly, the reporter strain lacks a functional promotor for genes encoding for spectinomycin resistance (*aadA*) and fluorescence (GFP). The donor DNA carrying the functional promotor was generated by PCR using the pCLT cloning vector as template (Mantilla-Calderon et al., 2019). The primer set of 5′-

ATT ATT GAA TTC GGT AGA GCC GTT TAT GAA-3′ forward and 5′-TTT GCC CAC TAC CTT GGT GAT-3′, amplifies the necessary donor DNA (2.1 kbp), which following translocation into the cell, can integrate into the reporter strain's genome via homologous recombination (Mantilla-Calderon et al., 2019). Integration of the promoter carried by the donor DNA activates the transcription of the gene fusion, restoring spectinomycin resistance and fluorescence by *A. baylyi* ADP1 (Rizzi et al., 2008). In these assays, only the donor DNA was exposed to the UV/H_2O_2 treatment, and the reporter strain remained unexposed to ensure the change in natural transformation rates was strictly due to DNA integrity and not any potential damage to the reporter strain. The donor DNA was spiked into AnMBR effluent at a final concentration of 2 µg/mL and exposed to irradiances of 0-311 mJ/cm^2 with H_2O_2 concentrations of 0, 10, and 30 mg/L. After the varied UV/H_2O_2 conditions, the donor DNA containing wastewater sample was transferred to a 2-mL centrifuge tube containing ca. 10^6 cells/mL of the reporter (*A. baylyi* ADP1) in LB broth, and the assay tubes were then placed in a shaker at 37 °C for a 24 h duration of transformation. Each set of tests were done with three sets of controls, namely one without donor DNA and exposed to UV/H_2O_2, one with respective H_2O_2 but kept in the dark for the given amount of time, and another without H_2O_2 and kept in the dark. To quantify transformation frequencies, 100 µL from the final assay tubes were plated on LB agar containing 100 µg/L of spectinomycin, 50 µg/L of kanamycin and 50 µg/L of rifampicin. The number of CFU that grew on these agar plates represent the transformant counts. These numbers of CFU were divided by the CFU on LB without spectinomycin but with kanamycin and rifampin, which represent the total number of cell counts. Each test was normalized by the dark control without H_2O_2 to compute fold-changes in natural transformation frequencies. Statistical differences were

Journal Pre-proof

263 determined by comparing the transformation frequencies at each irradiation level to those in the
264 dark using one-way ANOVA. All experiments were tested in biological triplicates.

265 *2.8 Water quality and parameters of MBR effluent*

266 Levels of COD, ammonia, and nitrate were measured using Hach kits based on manufacturer's
267 protocol, while turbidity was measured using a Hach turbidity meter (Loveland, CO, USA).
268 SUVA was determined by dividing absorbance at 254 nm, measured using a UV-3600 UV-Vis
269 spectrometer. Dissolved organic carbon (DOC) was determined using Shimadzu TOC-V total
270 organic carbon analyzer after passing water samples through a 0.45 µm filter. The pH of each
271 sample was measured using a Fisher Scientific Accumet AB150 benchtop meter. To determine
272 the effect of the overall water quality on hydroxyl radicals, nitrobenzene degradation was
273 measured, using high performance liquid chromatography (HPLC), throughout UV/H_2O_2
274 treatment. The presence of hydroxyl radicals with nitrobenzene will result in the degradation of
275 nitrobenzene to nitrophenols in a dose-dependent rate (Bhatia, 1975). The results are shown in
276 Figure S2 and the method is further detailed in Supporting Information Text 2.
277

278 **3. Results**

279 *3.1 Degradation of chemical contaminants*

280 At 10 and 30 mg/L H_2O_2 for all three CECs analyzed in this study, there was a fluence-
281 dependent increment in percent degradation of each compound (Figure 1). In the case of
282 atenolol, a beta blocker used to treat high blood pressure, there was no significant difference in
283 the degradation percentage with increasing fluence in the absence of H_2O_2. However, once H_2O_2
284 is added, hydroxyl radical formation significantly increased the degradation of atenolol
285 significantly after just 52 mJ/cm^2 albeit at 30 mg/L of H_2O_2 (Figure 1A). With increasing UV

Journal Pre-proof

286 fluence >104 mJ/cm^2, no difference in degradation percentage was observed when H_2O_2 was
287 increased from 10 to 30 mg/L. Average percent degradation at 311 mJ/cm^2 was also similar to
288 207 mJ/cm^2 for equal concentration of H_2O_2. The maximum degradation of atenolol was 97% at
289 311 mJ/cm^2 and 30 mg/L H_2O_2, but this percentage was not significantly different from the 96%
290 achieved at 311 mJ/cm^2 and 10 mg/L H_2O_2 (Table S5). For carbamazepine, an antiepileptic drug,
291 a significant improvement compared to 0 mg/L H_2O_2 was detected at 10 mg/L H_2O_2 after 207
292 mJ/cm^2 of UV exposure. Meanwhile a significant improvement in degradation upon increasing
293 H_2O_2 concentration from 0 mg/L to 30 mg/L was achieved at 52 mJ/cm^2 onwards. The maximum
294 degradation percentage of carbamazepine was 98%, achieved at 30 mg/L and 311 mJ/cm^2 but
295 this value was not different from the 97% achieved at 311 mJ/cm^2 and 10 mg/L H_2O_2 (Table S6).
296 The addition of H_2O_2 significantly increased the degradation of estrone, a female sex hormone,
297 even at the lowest irradiance of 52 mJ/cm^2. Thereafter, a maximum estrone degradation achieved
298 with UV/H_2O_2 was 92% at 30 mg/L H_2O_2 and 311 mJ/cm^2 (Table S7). The significance of the
299 addition of H_2O_2 is highlighted by the changes in the rate constants, assuming a second-order
300 reaction for all H_2O_2 concentrations. The *k*-values increased by 2.8, 2.0, and 1.39–fold for
301 atenolol, carbamazepine, and estrone, respectively, when increasing the H_2O_2 concentration from
302 10 to 30 mg/L at 311 mJ/cm^2 exposure (Table S8).
303
304 *3.2 Inactivation of ARB*
305 The inactivation of ARB *E. coli* PI7 and *K. pneumoniae* L7 in AnMBR effluent are shown in
306 Fig. 2. The slope determination and decay kinetics were calculated using the sampling points
307 between 0-52 mJ/cm^2, where consistent logarithmic decay was observed throughout all samples
308 with R^2 values all above 0.88. The average slopes from the inactivation curves of *E. coli* PI7

were -0.01, -0.12, and -0.13 log-removal per mJ/cm^2 for 0, 10 and 30 mg/L H_2O_2, respectively. The slopes were then used to calculate the irradiances needed for a 4-log inactivation of *E. coli* PI7 in the AnMBR effluent, which were 35.7, 25.2, and 25.4 mJ/cm^2 for 0, 10, and 30 mg/L H_2O_2. The addition of 10 mg/L significantly increased the inactivation rates of *E. coli* PI7 (Fig. 2A) based on slope comparisons (P-value = 0.02), however further increasing H_2O_2 concentration to 30 mg/L did not have a significant effect (P-value = 0.54). This same pattern can be seen when comparing the first-order rate constants. The average *k*-values for 0, 10 and 30 mg/L throughout the same 0-52 mJ/cm^2 period are 2.22 x 10^{-1}, 2.77 x 10^{-1}, 3.82 x 10^{-1} cm^2/mJ (Table S9). Following logarithmic decay, there was a disparity observed in the residual cellular concentration of *E. coli* PI7 (from 104-311 mJ/cm^2); being 2-log less when spiked with 10 mg/L compared to 0 mg/L (Fig. 2A).

The inactivation of *K. pneumoniae* L7 (Fig. 2B) was less altered by the addition of H_2O_2 compared to *E. coli* PI7. Only the use of 30 mg/L H_2O_2 had a significant effect of inactivation rates compared to 0 mg/L H_2O_2 (P-value = 0.02) when comparing slopes from 0-52 mJ/cm^2. However, the comparison slopes of 10 vs. 30 mg/L were not different. The decay kinetics from 0-52 mJ/cm^2 also slightly increased in the case of *K. pneumoniae* L7, whereby the *k*-values are 2.07 x 10^{-1}, 2.28 x 10^{-1}, 2.47 x 10^{-1} cm^2/mJ (Table S9). The required doses for a 4-log inactivation are 37.7, 33.1, and 31.6 mJ/cm^2 when using 0, 10, or 30 mg/L H_2O_2, respectively. Again, there was a disparity in average residual *K. pneumoniae* L7 cell concentrations from 104-311 mJ/cm^2, which differed by 0.9-log between 0 and 10 mg/L H_2O_2 (Fig. 2B).

3.3 Inactivation of extracellular DNA

Degradation of extracellular DNA associated with ARGs was quantified using qPCR (Fig. 3).

Journal Pre-proof

The ARGs were spiked at 10^6 copies/µL; the detection limit was 10^2 copies/µL. Degradation of ARGs was governed by UV exposure rather than the addition of H_2O_2 to UV. Without H_2O_2, there is a clear positive UV-dose dependent relationship and the degradation of $bla_{CTX\text{-}M15}$ (Fig. 3A), with a slope of 0.008 log-removal per mJ/cm^2 and an R^2 of 0.97 from 0-311 mJ/cm^2 and a *k*-value of 2.43 x 10^{-2} cm^2/mJ when normalized by irradiance (Table S10). Without H_2O_2, there was a maximum removal of 2.7-log at 311 mJ/cm^2 which was different to that achieved at 104 mJ/cm^2 of exposure but not to that achieved at 207 mJ/cm^2 (Table S11). The addition of 10 mg/L H_2O_2 did not significantly increase degradation of $bla_{CTX\text{-}M15}$ at any irradiance, however, at 311 mJ/cm^2 there was an average degradation of 3.3-log, which is a 0.6-log more degradation compared to 0 mg/L H_2O_2. Interestingly, at 30 mg/L H_2O_2 there was no statistical difference at any irradiance when comparing to 0 mg/L at any of the tested fluence as a pairwise comparison. Overall the maximum addition of H_2O_2 (30 mg/L) resulted in just a 1.2-fold increase in the rate constant *k* over the 311 mJ/cm^2, compared to 0 mg/L H_2O_2 (Table S10).

In the degradation of $bla_{NDM\text{-}1}$, the same UV concentration-dependent response was noted (Fig. 3B). At 0 mg/L H_2O_2, there was an increment in degradation with increase in UV dose following an average slope of 0.006 log-removal per mJ/cm^2 and an R^2 of 0.93 from 0-311 mJ/cm^2. A maximum removal of 2.1-log was achieved at 311 mJ/cm^2, however there was no significant increase in degradation after 104 mJ/cm^2 (Table S12). With the addition of 10 mg/L H_2O_2, there was no significant difference at any irradiance compared to 0 mg/L apart from 311 mJ/cm^2, where average degradation was increased to 2.9-log. Further increasing the H_2O_2 to 30 mg/L did not result in improvement in LRV compared to that at 10 mg/L nor 0 mg/L at each respective fluence. Lack of statistical significance in the changes of LRV as a result of increasing H_2O_2 concentration indicates that the removal of extracellular DNA was more governed by UV fluence

355 rather than H_2O_2 concentrations. The rate of that removal over the 311 mJ/cm^2 exposure,
356 represented by *k* increased slightly from 2.28 x 10^{-2} (0 mg/L H_2O_2) to 3.20 x 10^{-2} (10 mg/L
357 H_2O_2) and 3.34 x 10^{-2} (30 mg/L H_2O_2) as shown in Table S10.
358
359 *3.4 Mutagenicity effects of UV H_2O_2-treated water*
360 *Salmonella enterica* serovar Typhimurium TA98 and TA100 were used as mutagenicity assays
361 to assess possible frameshift and point mutations, respectively, using concentrated water samples
362 at each level of treatment (Fig. 4). The initial spiked effluent, prior to treatment showed no
363 difference to the negative control for either strain. Treated effluent without H_2O_2 did not illicit a
364 mutagenic response at any irradiance compared to the no-treatment sample in TA 100 (Fig. 4A).
365 There was however a significant increase in mutagenicity at 10 and 30 mg/L H_2O_2 starting at 104
366 mJ/cm^2 (Table S13). The maximum mutagenic response of 1.7-fold was observed after 311
367 mJ/cm^2 and 30 mg/L H_2O_2 in TA100. Furthermore, our results found no significant toxicity
368 increment due to UV/H_2O_2 treatment for all tested conditions using TA98 (Fig. 4B, Table S14).
369
370 *3.5. Transformability of DNA*
371 Although there was increase in mutagenicity associated with the treated wastewater matrix
372 (section 3.4), there was likewise a positive UV dose-response in DNA damage that further
373 prevented successful natural transformation of extracellular DNA that are present (Fig 5).
374 Without H_2O_2, the natural transformation frequency reported at 311 mJ/cm^2 UV exposure was
375 0.3-fold compared to dark control, which was significantly different to all other irradiances
376 without H_2O_2. The addition of 10 mg/L H_2O_2 resulted in a 0.2-fold induction that was not
377 different to UV alone at 311 mJ/cm^2 (Table S15). The addition of 30 mg/L H_2O_2 resulted in a

Journal Pre-proof

Journal Pre-proof

significant difference in transformation fold-induction to 0 mg/L H_2O_2 at every irradiance (Fig. 5). At the maximum tested irradiance, there was a 0.05-fold induction in natural transformation, or a 1.34 log reduction compared to the dark controls.

3.6. Water quality

Both ammonia and COD were oxidized by H_2O_2, and the oxidation increased with UV fluence (Table 1). The ammonia concentration was slightly reduced when exposed to 52-311 mJ/cm^2, although the difference was insignificant compared to untreated sample. The COD level reduced by 72% after UV/H_2O_2. Both turbidity and SUVA also decreased after UV/H_2O_2 exposure on AnMBR effluent, hence resulting in improved transmittance of the treated effluent. As AnMBR effluent was derived after a microfiltration membrane, the initial transmittance of 72% suggests suitability for UV/H_2O_2 treatment. However, a scavenging effect for the hydroxyl radicals generated from H_2O_2 was observed for the AnMBR effluent (Fig. S2). At 10 mg/L H_2O_2, the amount of nitrobenzene was significantly higher in the AnMBR effluent than that detected in MilliQ water at > 207 mJ/cm^2 (P-value = 0.043), indicating a corresponding lower degradation of nitrobenzene in AnMBR effluent than MilliQ could be due to the scavenging effect of organic constituents in the treated wastewater.

4. Discussion

AnMBR is increasingly being considered as a sustainable technology for treating municipal wastewaters. Recent demonstrations of several pilot-scale AnMBR in Spain, Italy, Korea (Foglia et al., 2020; Martinez-Sosa et al., 2012; Shin et al., 2014) reported a LRV of > 4 -log for coliforms (Foglia et al., 2020; Peña et al., 2019), which would not be sufficient to meet the

requirement for reuse purposes. Despite good LRV achieved by AnMBR alone, most guidelines still require the tertiary treated wastewater to be disinfected prior to reuse and that certain contaminants (e.g. dioxane) would have to be removed by no less than 0.5-log to meet the California Code of Regulations (CCR) Tittle 22. AnMBR would therefore have to be coupled with disinfection strategy in order for it to be used as one of the mainstream technologies to treat municipal wastewater.

When choosing an appropriate alternative disinfection strategy, consideration of the (i) practicality, (ii) efficacy of a broad range of contaminant removal, and (iii) minimal DBP formation (and hence low mutagenicity and horizontal gene transfer rates) would be of great importance. Ranking well in the three evaluated parameters would include UV/H_2O_2, O_3/H_2O_2, and UV/Cl_2 (von Gunten, 2018). Strong oxidants such as ozone or OH radicals consume DBP-forming precursors, lowering the risk arising from DBP formation by technologies such as UV/H_2O_2 and O_3/H_2O_2. While O_3/H_2O_2 has been shown to be more economic for the removal of CECs (Katsoyiannis et al., 2011), the main drawback for ozone-based treatment in bromide-containing waters is the formation of bromate (Von Gunten and Hoigne, 1994). Albeit, in ammonia-containing waters like that of AnMBR effluent quench HOBr, a bromate intermediate, lowering bromate formation by up to 4-fold (Buffle et al., 2004; Soltermann et al., 2017). This process, however, requires specific conditions including an oxidative treatment step (chlorine/ozone) and minimizing OH-radicals (lowering pH) to ensure HOBr formation (Soltermann et al., 2017) (Soltermann et al., 2017). The use of ozone would therefore require optimization on-site and incur additional chemical costs for disinfection.

Although the transmittance of the AnMBR effluent was ca. 72% (Table 1) and that the spiking of contaminants (e.g. ARB) at high concentrations would cause aggregation and light

Journal Pre-proof

scattering, the results still showed a relatively high inactivation efficiency of both ARB (5 LRV) and ARG (2 LRV). This inactivation is mainly contributed by UV rather than H_2O_2, previously demonstrated in (Pablos et al., 2013), where UV-C treatment with and without H_2O_2 gave the same kinetic constant (2.30 min^{-1}). The inactivation efficiency achieved in this study agrees with that reported by previous studies which saw 6 LRV of ARB in filtered wastewater after 3 min (Serna-Galvis et al., 2018), and 1.5-3.6 LRV for ARG after 124mJ/cm^2 of UV-C/H_2O_2 treatment with 10 mg/L H_2O_2 in pure water after 125 mJ/cm^2 (Yoon et al., 2018). Our results show that particularly at higher exposure, there was a significant increase in total ARB inactivation. Following the addition of H_2O_2, there was an improvement in ARB inactivation, which agrees with another study that also saw a 1-3 log increase in bacterial inactivation in humic-containing surface waters at > 311 mJ/cm^2 (Alkan et al., 2007). However, this study observed slightly lower inactivation rates of ARGs with *k*-values of up to 3.34 x 10^{-2} compared to that observed earlier, namely k = 6.1 x 10^{-2} (Yoon et al., 2018) and k = 1.1 x 10^{-1} (Chang et al., 2017). Amplicon length and water quality are likely the main contributors to this discrepancy among the k-values.

In contrast, UV alone is not that effective against CECs and would require the addition of H_2O_2 for the purpose of removing pharmaceutical compounds (Kim et al., 2009). H_2O_2 is photolyzed to form hydroxyl radicals which react non-selectively with organic and inorganic compounds present in the wastewater matrix (Stefan, 2017). Possible radical scavengers present in the water effluent limit the applicability of AOP, and generally wastewater with residual organics would require higher H_2O_2 concentrations to achieve effective degradation of CECs (Rosario-Ortiz et al., 2010). Furthermore, in this study, there was also scavenging by methanol, which was introduced as the solvent for the CECs. After spiking, there was 0.19 mM methanol in the AnMBR effluent which is oxidized and consumed relatively quickly by the OH radicals. This

would mean that higher UV irradiances might also be needed under these circumstances. Nevertheless, with 207 mJ/cm^2 and 10 mg/L of H_2O_2, we were able to achieve 90% reduction of the pharmaceutical compounds which was comparable to a study by Rosario Ortiz et al 2009, where they observed a >90% degradation of atenolol and carbamazepine from tertiary effluent with similar UV transmittance albeit with 20 mg/L H_2O_2 and 500 mJ/cm^2 (Rosario-Ortiz et al., 2010).

Although this study only measured degradation and removal of the parent compound, it is well established that transformation products form as a result of both oxidation (Lee and Von Gunten, 2016) and photodegradation (Fatta-Kassinos et al., 2011). We observed that regardless of the fate of these CECs, there was a slight increase in mutagenicity arising from point mutations which was not observed prior to disinfection. Mutagenicity has been demonstrated to increase natural transformation among competent bacteria (Augsburger et al., 2019; Mantilla-Calderon et al., 2019). Despite components of UV/H_2O_2 promoting the transfer of genetic components due to increase mutagenicity, there was no observed increase in the transformation frequency (Figure 5). This is likely due to the damage of extracellular DNA by UV exposure, which can preemptively inhibit successful HGT (Augsburger et al., 2019; Chang et al., 2017; He et al., 2019) and has its positive implications for the potential spread of antibiotic resistance and/or gaining of new functional traits. In this study, we only consider inactivation rates of extracellular DNA exclusively, ignoring intracellular DNA which has been shown to have slower inactivation kinetics (McKinney and Pruden, 2012). In (McKinney and Pruden, 2012), it was demonstrated that after 100 mJ/cm^2 of UV-C irradiance of four different genes, there was an average 0.14 LRV increase in removal of extracellular genes compared to its intracellular equivalent, suggesting that our described ability to inactivate extracellular DNA and

Journal Pre-proof

detrimentally affect transformation may not happen at the same efficiency for intracellular DNA. Similarly, McKinney and Pruden showed that the LRV achieved by UV-C varied among the four genes, further suggesting that the size and nucleic acid composition of the DNA to be inactivated by UV-C are important factors that can also affect the efficacy.

While the findings in this study suggest that UV/H_2O_2 is effective against CECs, ARB and ARGs, these experiments were performed in a batch mode with significantly smaller volumes and higher initial concentrations than that present in full-scale operations. While higher CEC and cellular concentrations help with detection resolution, it also worsened water quality. In real wastewater, relative rate constants of the dissolved fraction (CECs, dissolved organic matter (DOM), cells, etc.) with either UV or OH-radical will determine the degradation rate and this will heavily vary on a case-to-case basis. For this reason we see large variations in removal of chemical contaminants in real wastewater (Krzeminski et al., 2019), possibly due to differing concentrations of these contaminants. Furthermore, the effluent used in this study came from an AnMBR equipped with at 0.3 μm nominal pore size microfilter, and was sequentially filtered by a 0.45 μm syringe filter to minimize contamination risk for our culture-based quantification methods. We acknowledge such procedures are equivalent to a double stage filtration process that would lower the turbidity of the water and improve UV efficacy. Hence, translated applications of UV/H2O2 to disinfect AnMBR effluent in full-scale systems would require further evaluation. Finally, when translating for full-scale systems, batch mode disinfection such as the one demonstrated in this study would be impractical due to the need for a large reactor footprint. Thus, adjustments to the needed fluence and concentrations may be needed to achieve the reported removal values. This can be done for instance, by allowing a suitable hydraulic flow

Journal Pre-proof

rate through a flow-through UV reactor to ensure sufficient contact time between the UV/H_2O_2 and the AnMBR effluent.

5. Conclusions

In this study, we demonstrated the use of UV/H_2O_2 as a potential strategy to reduce the levels of CECs, ARB and ARGs that are present in the ammonia-rich AnMBR effluent. In such water matrix, ARB and ARG inactivation was driven mainly by UV-C_{254nm} exposure. The addition of H_2O_2 to UV disinfection was required to achieve efficient CECs degradation. While 10 mg/L H_2O_2 significantly improved the degradation of trace CECs compared to UV alone, increasing the H_2O_2 concentration to 30 mg/L did not cause significant improvement in the degradation efficiency. Although there was an increase in mutagenicity of the treated waters likely due to the products formed from the reaction between CECs and H_2O_2, there was no changes in the natural transformation rates after UV/H_2O_2. These observations suggest that UV/H_2O_2 can act as an efficient and safe disinfection strategy in removing both biological and chemical contaminants from an ammonia rich AnMBR effluent. The proposed disinfection strategy also bypasses the need to remove ammonia from the AnMBR effluent, hence allowing one to use such high-quality treated effluent as liquid fertilizers for food production.

6. Acknowledgement

This study was supported by KAUST Center Applied Research Funding FCC/1/1971-32-01 and Center of Excellence for NEOM Research flagship projects REI/1/4178-03-01 awarded to P.Y.-H.

Journal Pre-proof

516

Journal Pre-proof

Journal Pre-proof

517 **Table 1.** Water quality parameters of the AnMBR effluent before and after spiking with all
518 contaminants and during AOP treatment supplemented 10 mg/L H_2O_2.

	pH	Ammonia (mg/L NH_3-N)	COD (mg/L)	DOC (mg/L)	Turbidity (NTU)	SUVA (m^{-1} mg^{-1} L)	Transmittance (254nm)
AnMBR effluent	8.02 (± 0.04)	20.06 (± 1.46)	24.5 (± 3.39)	12.09 (± 2.46)	1.32 (± 0.25)	0.47 (± 0.20)	88 % (± 2.14)
After spiking	8.30 (± 0.13)	19.9 (± 0.4)	125.5 (± 0.57)	39.2 (± 3.42)	4.54 (± 0.35)	0.36 (± 0.09)	72 % (± 1.56)
52 mJ/cm²	8.77 (± 0.05)	16.2 (± 0.4)	77.6 (± 9.26)	23.4 (± 4.16)	4.59 (± 0.07)	0.35 (± 0.30)	87 % (± 6.94)
104 mJ/cm²	8.24 (± 0.16)	16.7 (± 1.9)	57.5 (± 3.54)	16.7 (± 2.91)	2.40 (± 1.03)	0.21 (± 0.09)	92 % (± 2.69)
207 mJ/cm²	8.31 (± 0.08)	14.9 (± 0.4)	41.5 (± 7.78)	14.4 (± 3.24)	2.93 (± 0.62)	0.24 (± 0.08)	92 % (± 3.13)
311 mJ/cm²	8.37 (± 0.06)	13.7 (± 3.6)	35 (± 8.49)	14.2 (± 5.14)	2.32 (± 0.62)	0.23 (± 0.20)	93 % (± 1.86)

519
520
521
522

Journal Pre-Proof

Journal Pre-proof

Figure legends

Figure 1. Percent degradation of **(A)** atenolol, **(B)** carbamazepine, and **(C)** estrone as a function of both fluence (i.e., 0, 52, 104, 207 and 311 mJ/cm^2) and H_2O_2 concentrations (i.e., 0, 10 and 30 mg/L).

Figure 2. Inactivation curves of **(A)** *E.coli* PI7 and **(B)** *K. pneumoniae* L7 as a function of UV exposure at varying H_2O_2 concentrations.

Figure 3. Inactivation **of (A)** bla$_{CTX\text{-}M\text{-}15}$ and **(B)** bla$_{NDM\text{-}1}$ genes as a function of fluence and at varying H_2O_2 concentrations.

Figure 4. Mutagenic response **(A)** TA100 and **(B)** TA98 as a function of exposure to 20X concentrated water samples collected after no treatment and various UV fluence with 10 mg/L H_2O_2. Positive control denotes mutagenic response upon exposure to 100 μg/mL sodium azide.

Figure 5. Integrity of extracellular DNA damage assessed by natural transformation assay. Extracellular DNA was exposed to various UV fluence with varying concentrations of H_2O_2.

Journal Pre-proof

Journal Pre-proof

548 **References**
549
550 Al-Jasser, A. 2011. Saudi wastewater reuse standards for agricultural irrigation: Riyadh
551 treatment plants effluent compliance. Journal of King Saud University-Engineering
552 Sciences 23(1), 1-8.
553 Alkan, U., Teksoy, A., Atesli, A. and Baskaya, H.S. 2007. Efficiency of the UV/H2O2 process for
554 the disinfection of humic surface waters. Journal of environmental science and health,
555 Part A 42(4), 497-506.
556 Augsburger, N., Mantilla-Calderon, D., Daffonchio, D. and Hong, P.-Y. 2019. Acquisition of
557 Extracellular DNA by Acinetobacter baylyi ADP1 in response to Solar and UV-C254nm
558 Disinfection. Environmental science & technology 53(17), 10312-10319.
559 Bhatia, K. 1975. Hydroxyl radical induced oxidation of nitrobenzene. The Journal of Physical
560 Chemistry 79(10), 1032-1038.
561 Bolton, J.R. and Linden, K.G. 2003. Standardization of methods for fluence (UV dose)
562 determination in bench-scale UV experiments. Journal of environmental engineering
563 129(3), 209-215.
564 Bond, T., Huang, J., Templeton, M.R. and Graham, N. 2011. Occurrence and control of
565 nitrogenous disinfection by-products in drinking water–a review. Water research 45(15),
566 4341-4354.
567 Buffle, M.-O., Galli, S. and von Gunten, U. 2004. Enhanced bromate control during ozonation:
568 the chlorine-ammonia process. Environmental science & technology 38(19), 5187-5195.
569 Chang, P.H., Juhrend, B., Olson, T.M., Marrs, C.F. and Wigginton, K.R. 2017. Degradation of
570 extracellular antibiotic resistance genes with UV254 treatment. Environmental Science
571 & Technology 51(11), 6185-6192.
572 Cheng, H., Guan, Q., Villalobos, L.F., Peinemann, K.-V., Pain, A. and Hong, P.-Y. 2019.
573 Understanding the antifouling mechanisms related to copper oxide and zinc oxide
574 nanoparticles in anaerobic membrane bioreactors. Environmental Science: Nano 6(11),
575 3467-3479.
576 Cheng, H. and Hong, P.-Y. 2017. Removal of antibiotic-resistant bacteria and antibiotic
577 resistance genes affected by varying degrees of fouling on anaerobic microfiltration
578 membranes. Environmental science & technology 51(21), 12200-12209.
579 Choi, K.J., Kim, S.G., Kim, C.W. and Park, J.K. 2006. Removal efficiencies of endocrine disrupting
580 chemicals by coagulation/flocculation, ozonation, powdered/granular activated carbon
581 adsorption, and chlorination. Korean Journal of Chemical Engineering 23(3), 399-408.
582 Doetsch, P.W., Zastawny, T.H., Martin, A.M. and Dizdaroglu, M. 1995. Monomeric Base
583 Damage Products from Guanine, Adenine, and Thymine Induced by Exposure of DNA to
584 Ultraviolet Radiation. Biochemistry 34(3), 737-742.
585 Fatta-Kassinos, D., Vasquez, M.I. and Kümmerer, K. 2011. Transformation products of
586 pharmaceuticals in surface waters and wastewater formed during photolysis and
587 advanced oxidation processes–degradation, elucidation of byproducts and assessment
588 of their biological potency. Chemosphere 85(5), 693-709.
589 Fiorentino, A., Ferro, G., Alferez, M.C., Polo-López, M.I., Fernández-Ibañez, P. and Rizzo, L.
590 2015. Inactivation and regrowth of multidrug resistant bacteria in urban wastewater

after disinfection by solar-driven and chlorination processes. Journal of Photochemistry and Photobiology B: Biology 148, 43-50.

Foglia, A., Akyol, Ç., Frison, N., Katsou, E., Eusebi, A.L. and Fatone, F. 2020. Long-term operation of a pilot-scale anaerobic membrane bioreactor (AnMBR) treating high salinity low loaded municipal wastewater in real environment. Separation and Purification Technology 236, 116279.

Goldstein, M., Shenker, M. and Chefetz, B. 2014. Insights into the uptake processes of wastewater-borne pharmaceuticals by vegetables. Environmental science & technology 48(10), 5593-5600.

Guo, M.-T., Yuan, Q.-B. and Yang, J. 2015. Distinguishing effects of ultraviolet exposure and chlorination on the horizontal transfer of antibiotic resistance genes in municipal wastewater. Environmental science & technology 49(9), 5771-5778.

He, H., Zhou, P., Shimabuku, K.K., Fang, X., Li, S., Lee, Y. and Dodd, M.C. 2019. Degradation and Deactivation of Bacterial Antibiotic Resistance Genes during Exposure to Free Chlorine, Monochloramine, Chlorine Dioxide, Ozone, Ultraviolet Light, and Hydroxyl Radical. Environmental science & technology.

Hrudey, S.E. 2009. Chlorination disinfection by-products, public health risk tradeoffs and me. Water research 43(8), 2057-2092.

Huang, H., Wu, Q.-Y., Tang, X., Jiang, R. and Hu, H.-Y. 2016. Formation of haloacetonitriles and haloacetamides and their precursors during chlorination of secondary effluents. Chemosphere 144, 297-303.

Katsoyiannis, I.A., Canonica, S. and von Gunten, U. 2011. Efficiency and energy requirements for the transformation of organic micropollutants by ozone, O3/H2O2 and UV/H2O2. Water research 45(13), 3811-3822.

Kim, I., Yamashita, N. and Tanaka, H. 2009. Performance of UV and UV/H2O2 processes for the removal of pharmaceuticals detected in secondary effluent of a sewage treatment plant in Japan. Journal of Hazardous Materials 166(2-3), 1134-1140.

Kim, M., Guerra, P., Shah, A., Parsa, M., Alaee, M. and Smyth, S. 2014. Removal of pharmaceuticals and personal care products in a membrane bioreactor wastewater treatment plant. Water science and technology 69(11), 2221-2229.

Krzeminski, P., Tomei, M.C., Karaolia, P., Langenhoff, A., Almeida, C.M.R., Felis, E., Gritten, F., Andersen, H.R., Fernandes, T. and Manaia, C.M. 2019. Performance of secondary wastewater treatment methods for the removal of contaminants of emerging concern implicated in crop uptake and antibiotic resistance spread: A review. Science of the Total Environment 648, 1052-1081.

Lee, Y., Gerrity, D., Lee, M., Gamage, S., Pisarenko, A., Trenholm, R.A., Canonica, S., Snyder, S.A. and Von Gunten, U. 2016. Organic contaminant abatement in reclaimed water by UV/H2O2 and a combined process consisting of O3/H2O2 followed by UV/H2O2: prediction of abatement efficiency, energy consumption, and byproduct formation. Environmental science & technology 50(7), 3809-3819.

Lee, Y. and Von Gunten, U. 2016. Advances in predicting organic contaminant abatement during ozonation of municipal wastewater effluent: reaction kinetics, transformation products, and changes of biological effects. Environmental Science: Water Research & Technology 2(3), 421-442.

Journal Pre-proof

635 Lei, H. and Snyder, S.A. 2007. 3D QSPR models for the removal of trace organic contaminants
636 by ozone and free chlorine. Water research 41(18), 4051-4060.
637 Ling, T.L., Ahmad, M. and Heng, L.Y. 2011. Quantitative Determination of Ammonium Ion in
638 Aqueous Environment Using Riegler's Solution and Artificial Neural Network. Sains
639 Malaysiana 40(10), 1105-1113.
640 Ling, T.L., Ahmad, M. and Heng, L.Y. 2013. UV-vis spectrophotometric and artificial neural
641 network for estimation of ammonia in aqueous environment using cobalt (II) ions.
642 Analytical Methods 5(23), 6709-6714.
643 Malchi, T., Maor, Y., Tadmor, G., Shenker, M. and Chefetz, B. 2014. Irrigation of root
644 vegetables with treated wastewater: evaluating uptake of pharmaceuticals and the
645 associated human health risks. Environmental science & technology 48(16), 9325-9333.
646 Mantilla-Calderon, D., Jumat, M.R., Wang, T., Ganesan, P., Al-Jassim, N. and Hong, P.-Y. 2016.
647 Isolation and characterization of NDM-positive Escherichia coli from municipal
648 wastewater in Jeddah, Saudi Arabia. Antimicrobial agents and chemotherapy 60(9),
649 5223-5231.
650 Mantilla-Calderon, D., Plewa, M.J., Michoud, G., Fodelianakis, S., Daffonchio, D. and Hong, P.
651 2019. Water disinfection byproducts increase natural transformation rates of
652 environmental DNA in Acinetobacter baylyi ADP1. Environmental Science & Technology.
653 Maron, D.M. and Ames, B.N. 1983. Revised methods for the Salmonella mutagenicity test.
654 Mutation Research/Environmental Mutagenesis and Related Subjects 113(3-4), 173-215.
655 Martinez-Sosa, D., Helmreich, B. and Horn, H. 2012. Anaerobic submerged membrane
656 bioreactor (AnSMBR) treating low-strength wastewater under psychrophilic
657 temperature conditions. Process Biochemistry 47(5), 792-798.
658 McKinney, C.W. and Pruden, A. 2012. Ultraviolet disinfection of antibiotic resistant bacteria
659 and their antibiotic resistance genes in water and wastewater. Environmental science &
660 technology 46(24), 13393-13400.
661 Miklos, D.B., Remy, C., Jekel, M., Linden, K.G., Drewes, J.E. and Hübner, U. 2018. Evaluation of
662 advanced oxidation processes for water and wastewater treatment–A critical review.
663 Water research 139, 118-131.
664 Munir, M., Wong, K. and Xagoraraki, I. 2011. Release of antibiotic resistant bacteria and genes
665 in the effluent and biosolids of five wastewater utilities in Michigan. Water research
666 45(2), 681-693.
667 Nieuwenhuijsen, M.J., Toledano, M.B., Eaton, N.E., Fawell, J. and Elliott, P. 2000. Chlorination
668 disinfection byproducts in water and their association with adverse reproductive
669 outcomes: a review. Occupational and environmental medicine 57(2), 73-85.
670 Okuda, T., Kobayashi, Y., Nagao, R., Yamashita, N., Tanaka, H., Tanaka, S., Fujii, S., Konishi, C.
671 and Houwa, I. 2008. Removal efficiency of 66 pharmaceuticals during wastewater
672 treatment process in Japan. Water Science and Technology 57(1), 65-71.
673 Pablos, C., Marugan, J., van Grieken, R. and Serrano, E. 2013. Emerging micropollutant
674 oxidation during disinfection processes using UV-C, UV-C/H2O2, UV-A/TiO2 and UV-
675 A/TiO2/H2O2. Water research 47(3), 1237-1245.
676 Park, K.-Y., Choi, S.-Y., Lee, S.-H., Kweon, J.-H. and Song, J.-H. 2016. Comparison of formation
677 of disinfection by-products by chlorination and ozonation of wastewater effluents and
678 their toxicity to Daphnia magna. Environmental Pollution 215, 314-321.

Journal Pre-proof

679 Peña, M., do Nascimento, T., Gouveia, J., Escudero, J., Gómez, A., Letona, A., Arrieta, J. and Fdz-
680 Polanco, F. 2019. Anaerobic submerged membrane bioreactor (AnSMBR) treating
681 municipal wastewater at ambient temperature: Operation and potential use for
682 agricultural irrigation. Bioresource technology 282, 285-293.
683 Rizzi, A., Pontiroli, A., Brusetti, L., Borin, S., Sorlini, C., Abruzzese, A., Sacchi, G.A., Vogel, T.M.,
684 Simonet, P. and Bazzicalupo, M. 2008. Strategy for in situ detection of natural
685 transformation-based horizontal gene transfer events. Applied and environmental
686 microbiology 74(4), 1250-1254.
687 Rosario-Ortiz, F.L., Wert, E.C. and Snyder, S.A. 2010. Evaluation of UV/H2O2 treatment for the
688 oxidation of pharmaceuticals in wastewater. Water research 44(5), 1440-1448.
689 Serna-Galvis, E.A., Salazar-Ospina, L., Jiménez, J.N., Pino, N.J. and Torres-Palma, R.A. 2018.
690 Elimination of carbapenem resistant Klebsiella pneumoniae in water by UV-C, UV-
691 C/persulfate and UV-C/H2O2. Evaluation of response to antibiotic, residual effect of the
692 processes and removal of resistance gene. Journal of Environmental Chemical
693 Engineering, 102196.
694 Shah, A.D. and Mitch, W.A. 2012. Halonitroalkanes, halonitriles, haloamides, and N-
695 nitrosamines: a critical review of nitrogenous disinfection byproduct formation
696 pathways. Environmental Science & Technology 46(1), 119-131.
697 Shin, C., McCarty, P.L., Kim, J. and Bae, J. 2014. Pilot-scale temperate-climate treatment of
698 domestic wastewater with a staged anaerobic fluidized membrane bioreactor (SAF-
699 MBR). Bioresource Technology 159, 95-103.
700 Sinha, R.P. and Häder, D.-P. 2002. UV-induced DNA damage and repair: a review.
701 Photochemical & Photobiological Sciences 1(4), 225-236.
702 Soltermann, F., Abegglen, C., Tschui, M., Stahel, S. and Von Gunten, U. 2017. Options and
703 limitations for bromate control during ozonation of wastewater. Water research 116,
704 76-85.
705 Stefan, M.I. (2017) Advanced oxidation processes for water treatment: fundamentals and
706 applications, IWA publishing.
707 Subedi, B. and Kannan, K. 2015. Occurrence and fate of select psychoactive pharmaceuticals
708 and antihypertensives in two wastewater treatment plants in New York State, USA.
709 Science of the Total Environment 514, 273-280.
710 Toh, B.E., Bokhari, O., Kutbi, A., Haroon, M.F., Mantilla-Calderon, D., Zowawi, H.M. and Hong,
711 P.-Y. 2017. Occurrence of extended-spectrum beta-lactamase Gram-negative bacteria
712 among various types of produce results in different level of ingestion risks.
713 Verlicchi, P., Al Aukidy, M. and Zambello, E. 2012. Occurrence of pharmaceutical compounds in
714 urban wastewater: removal, mass load and environmental risk after a secondary
715 treatment—a review. Science of the total environment 429, 123-155.
716 von Gunten, U. 2018. Oxidation processes in water treatment: are we on track? Environmental
717 science & technology 52(9), 5062-5075.
718 Von Gunten, U. and Hoigne, J. 1994. Bromate formation during ozonization of bromide-
719 containing waters: interaction of ozone and hydroxyl radical reactions. Environmental
720 science & technology 28(7), 1234-1242.
721 WHO 2017 List of bacteria for which new antibiotics are urgently needed. GENEVA, W. (ed),
722 Newsroom Detail.

Journal Pre-proof

Journal Pre-proof

723 Wu, X., Conkle, J.L., Ernst, F. and Gan, J. 2014. Treated wastewater irrigation: uptake of
724 pharmaceutical and personal care products by common vegetables under field
725 conditions. Environmental science & technology 48(19), 11286-11293.
726 WWAP 2015. The Un World Water Development Report 2015. Water for a Sustainable World.
727 WWAP 2019 The United Nations World Water Development Report 2019: Leaving No One
728 Behind, UNESCO Paris.
729 Yang, X., Fan, C., Shang, C. and Zhao, Q. 2010. Nitrogenous disinfection byproducts formation
730 and nitrogen origin exploration during chloramination of nitrogenous organic
731 compounds. Water research 44(9), 2691-2702.
732 Yoon, Y., Dodd, M.C. and Lee, Y. 2018. Elimination of transforming activity and gene
733 degradation during UV and UV/H 2 O 2 treatment of plasmid-encoded antibiotic
734 resistance genes. Environmental Science: Water Research & Technology 4(9), 1239-
735 1251.
736 Yuan, Q.-B., Guo, M.-T. and Yang, J. 2015. Fate of antibiotic resistant bacteria and genes during
737 wastewater chlorination: implication for antibiotic resistance control. PLoS One 10(3),
738 e0119403.
739
740
741

Journal Pre-proof

Journal Pre-proof

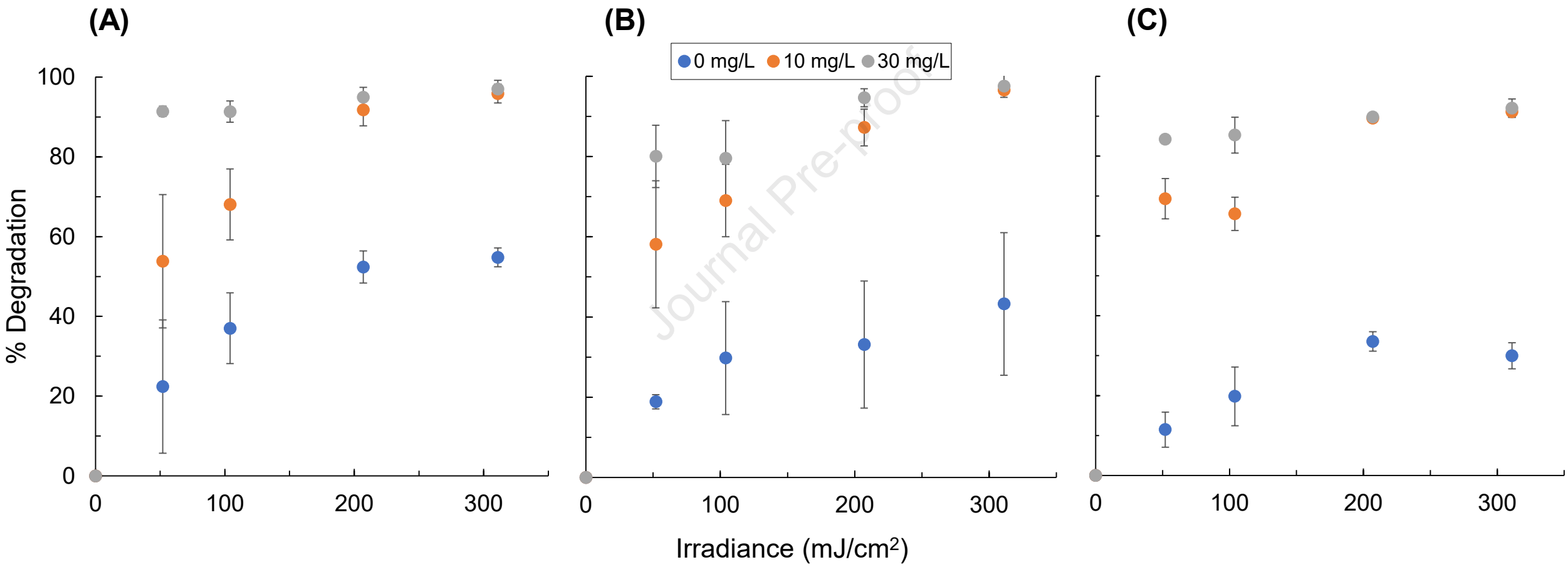

Journal Pre-proof

Journal Pre-proof

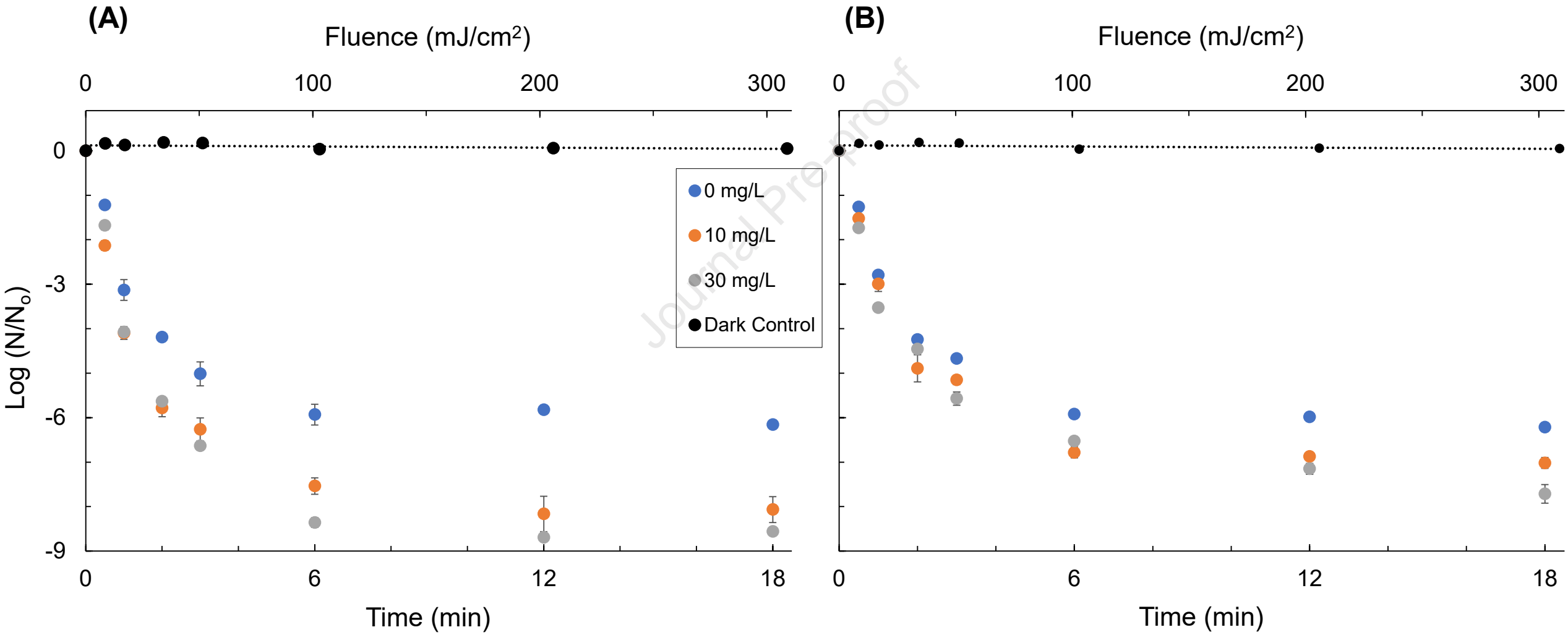

Journal Pre-proof

Journal Pre-proof

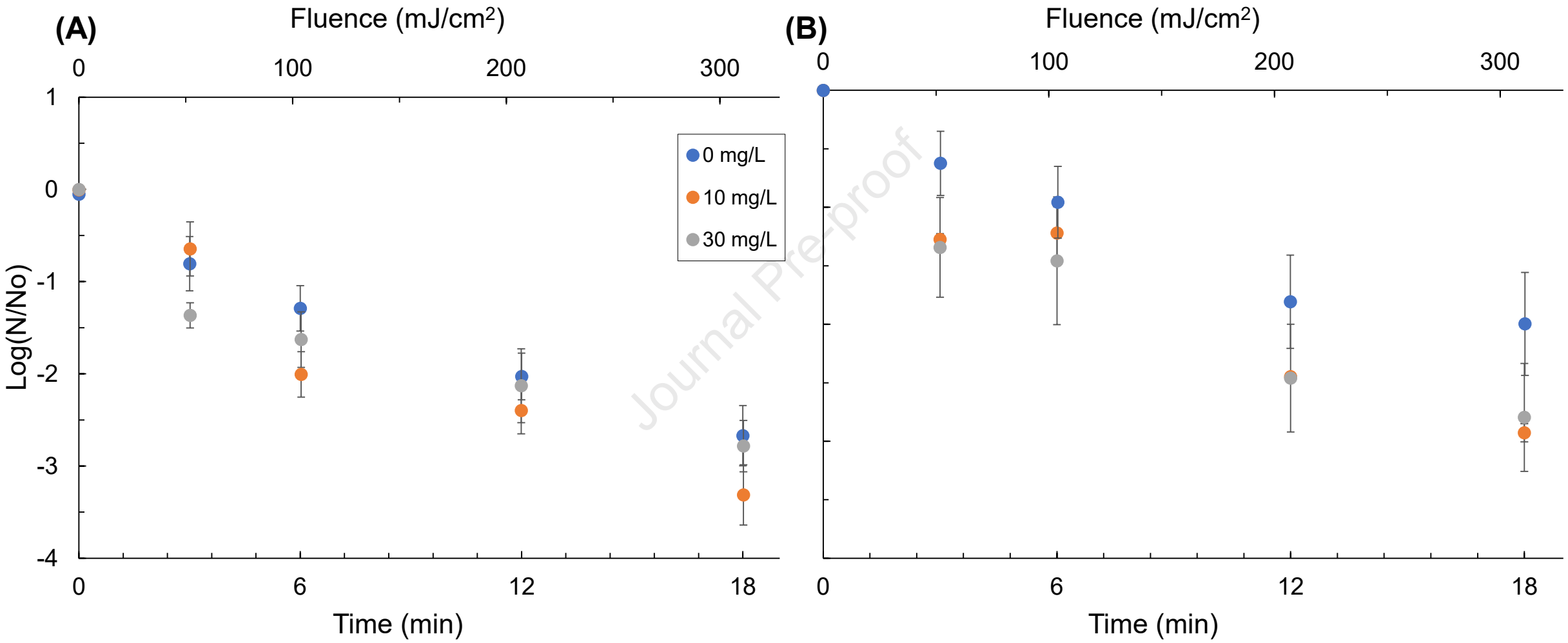

Journal Pre-proof

Journal Pre-proof

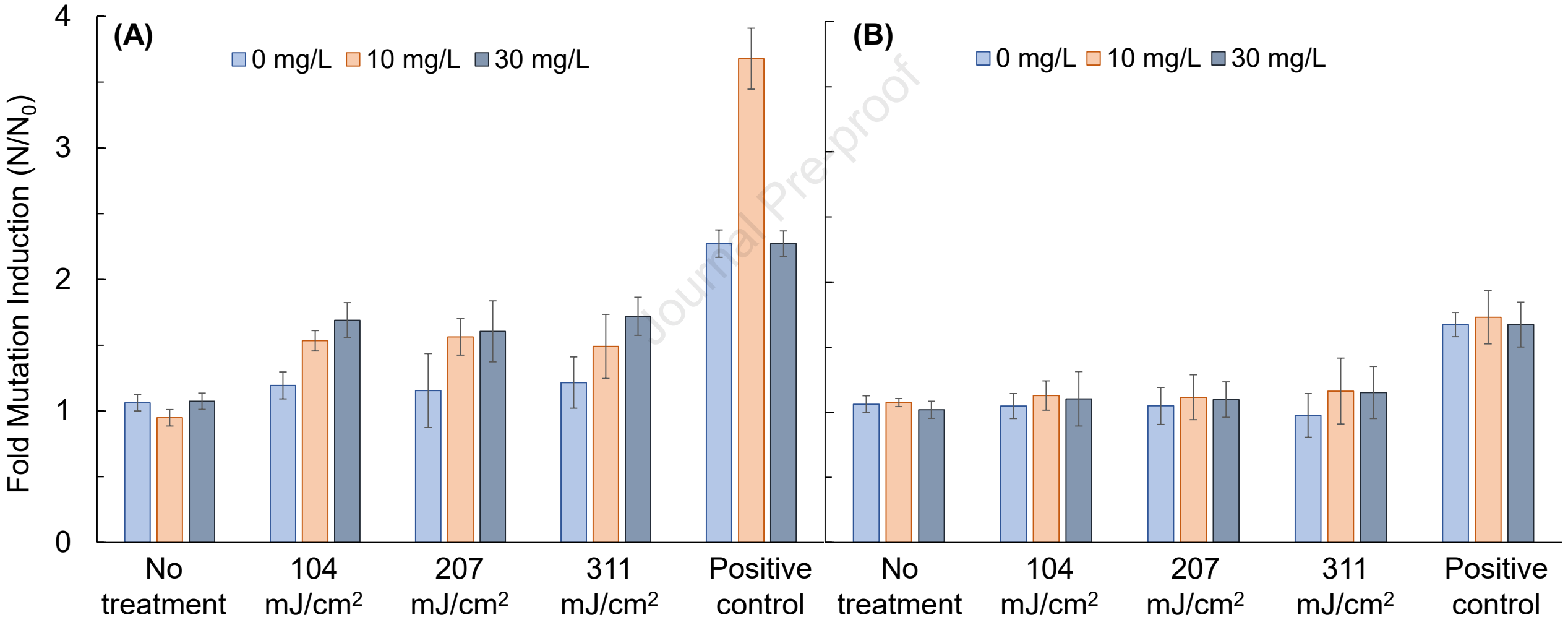

Journal Pre-proof

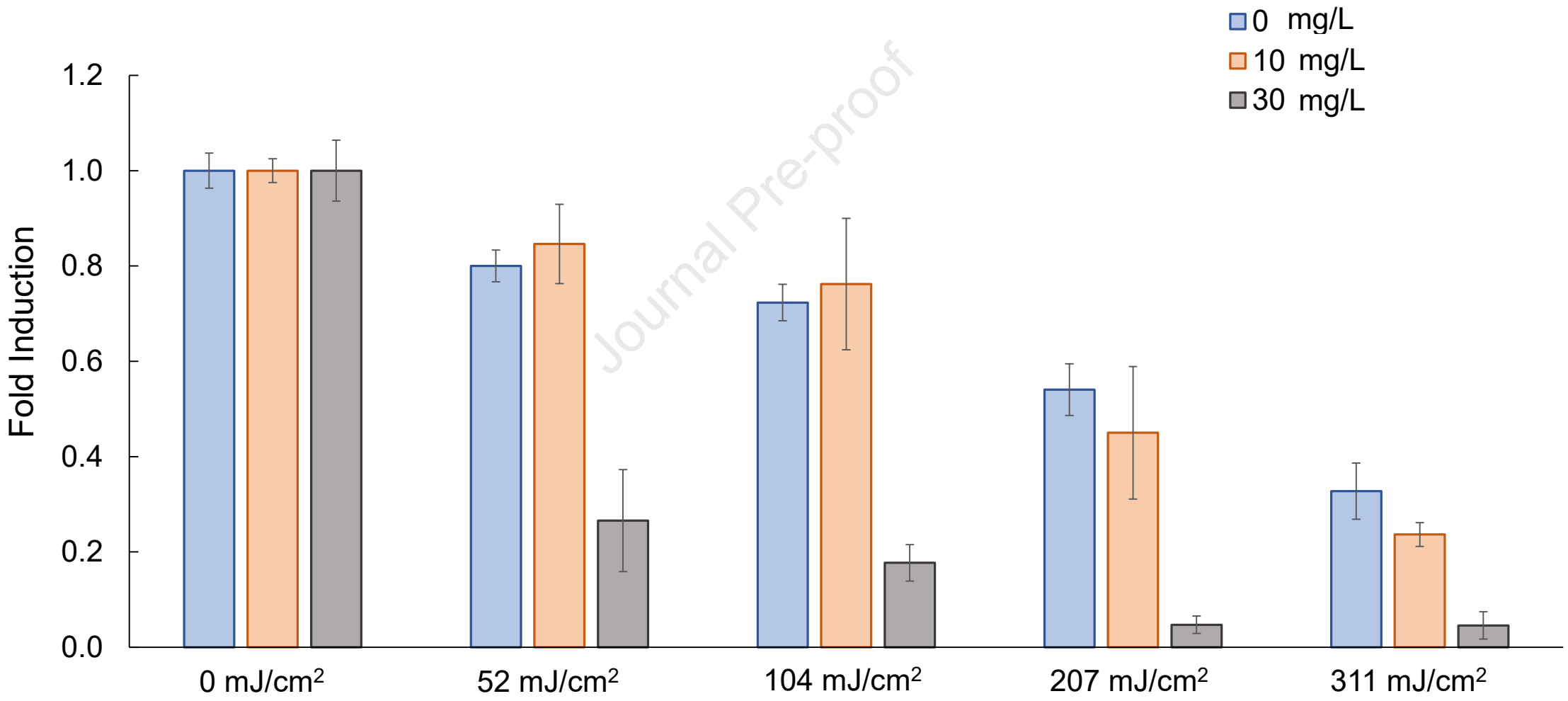

Journal Pre-proof

Journal Pre-proof

Highlights

- 10 mg/L H_2O_2 and 400 mJ/cm^2 UV removes 1-log of chemical contaminants from anaerobic effluent
- UV was the main factor to remove antibiotic resistant bacteria (ARB) and genes rather than H_2O_2
- > 5-log removal of ARB was achieved at > 400 mJ/cm^2 and > 10 mg/L H_2O_2
- UV/H_2O_2 significantly increased mutagenicity after 200 mJ/cm^2
- Extracellular DNA removed by > 2-log and cannot be transformed into competent host
- Various aspects of water quality improved after disinfecting with UV/ H_2O_2

Journal Pre-proof

Journal Pre-proof

Declaration of interests

☒ The authors declare that they have no known competing financial interests or personal relationships that could have appeared to influence the work reported in this paper.

☐The authors declare the following financial interests/personal relationships which may be considered as potential competing interests:

Journal Pre-proof